7. Seismology

Michel Campillo, Ludovic Margerin and Keiiti Aki

In recent years, the attention of seismologists has turned to the physics of multiple scattering of elastic waves in the Earth. Analysis of the records of ground motion at the surface of the Earth has allowed imaging of the interior of the planet at different scales, in the framework of the classical theory of elastodynamics. Seismic data consist of time series of the 3D motions recorded when the surface of the Earth is hit by mechanical waves. Seismic signals cover a frequency band typically between 0.01 and 100 Hz. The sources in most cases produce pulses which are very short with respect to the travel time of the waves.

The development of piecewise homogeneous Earth models has been a fundamental step forward, with important implications for studies of the Earth's dynamics, the origin of the magnetic field and the quantification of earthquakes. Whatever the particular technique for imaging in use (reflection seismic prospecting, body wave tomography or surface wave tomography), the objective has always been the determination of the local local properties of an effective medium that can be related to a particular constituent or geological unit. However, it was realized early that such models cannot account for all characteristics of seismic signals. Two major observations lead us to consider the effect of scattering by the inhomogeneity of the materials: the strong apparent attenuation of the seismic signals and the duration of the seismograms, which greatly exceeds the travel times of the direct waves. These late arrivals are called the seismic coda.

7.1 Specific Consequences of Elasticity

The equation of linear isotropic elasticity for the three components of the displacement $u_i(t, x_1, x_2, x_3), i = 1, 2, 3$, is

$$\rho \frac{\partial^2 u_i}{\partial t^2} = \frac{\partial}{\partial x_i}\left(\lambda \frac{\partial u_j}{\partial x_j}\right) + \frac{\partial}{\partial x_j}\left(\mu \frac{\partial u_j}{\partial x_i} + \mu \frac{\partial u_i}{\partial x_j}\right), \tag{7.1}$$

in which $\lambda(x_1, x_2, x_3)$ and $\mu(x_1, x_2, x_3)$ are the Lamé parameters and $\rho(x_1, x_2, x_3)$ is the density. In a homogeneous medium this equation reduces to two wave equations for the potentials: the scalar compressional potential φ and the vectorial shear potential ψ. These potentials are associated with the

longitudinal P wave and the transversely polarized S waves. They propagate with different velocities α and β respectively, and couple during a scattering event. Unlike what happens in classical optics or acoustics, the coupling is more complex than just a mixing of polarization channels, since two different waves and wave speeds are involved. This aspect has an interesting analogy in the recent study of light diffusion in nematic liquid crystals [79, 81, 82] (Sect. 1.4.3).

In the context of elastic-wave scattering, it is important to note that P to S and S to P conversions are not processes of equivalent strength. As demonstrated from the reciprocity theorem, for a single scattering event [302] (corrected in [303]), the scattering coefficients in terms of energy, g_{PS} and g_{SP}, are related by

$$\frac{g_{PS}}{g_{SP}} = 2\frac{\alpha^4}{\beta^4} . \tag{7.2}$$

This result indicates that at each diffraction event the energy is preferentially diffracted into shear waves. So the shear energy will finally dominate the diffuse field. This property has been used as an argument to limit the discussion on multiply scattered waves to the simplest case of shear waves. The observations confirm the prominence of shear waves in the late arrivals. Nevertheless, we shall show that a complete treatment of the elastic case is required.

7.2 1D Problem

The one-dimensional problem has been extensively studied since the shallow structure of the Earth can often be considered as a stack of thin layers with different densities and wave velocities that fluctuate randomly. This is particularly true for sedimentary structures from which hydrocarbons are extracted. In the long-wavelength limit, such a medium can be described by the effective anisotropic parameters [304]. For high-frequency waves, it has been noticed in seismic prospecting that the frequency content of a pulse propagating through a thin, layered structure changes drastically, resulting in the phenomenon known as "stratigraphic filtering". This effect is indeed of great practical importance in the signal processing of reflected pulses from deep reflectors. It would also be a valuable parameter to measure, if one could relate the apparent attenuation of the pulse to the statistical characteristics of the stratigraphy itself. This apparent attenuation is indeed directly associated with the localization length $\mathcal{L}$, although this terminology is not currently used in the seismological literature. The spatial decay is commonly characterized by the scattering quality factor $Q(f)$, originating from a confusing analogy with absorption attenuation. $Q(f)$ and $\mathcal{L}(f)$ are simply related by

$$\mathcal{L}(f) = \frac{Q(f)V_e}{\pi f}, \tag{7.3}$$

where V_e is the effective velocity and f the frequency.

7.2.1 Acoustic Waves

Multiple scattering in a layered structure was first studied for acoustic waves, corresponding to a scalar simplification in which the coupling between the two elastic potentials is neglected.

In 1971, O'Doherty and Anstey [305] proposed an expression relating the amplitude spectrum of the stratigraphic filter $A(\omega)$ for a vertically incident wave to the power spectrum of the reflection coefficient series $R(\omega)$ and the travel time t of the transmitted primary wave, in the form

$$A(\omega) = \exp[-R(\omega)t]. \tag{7.4}$$

This formula has been derived [306] in the context of the mean-field formalism. This method is based on the representation of the field by the sum of a mean field (in the sense of ensemble average) and a small fluctuating field. Weak fluctuations and a homogeneous background are assumed. The property of self-averaging is implicit in the use of this expression.

Asch et al. [307] give a comprehensive analysis of the properties of an acoustic signal reflected by a randomly layered medium that obeys the scaling property (see also Sect. 4.3)

$$a < \lambda < L, \tag{7.5}$$

where a is a characteristic length scale of the inhomogeneity (the thickness of the layers), λ the wavelength and L the thickness of the inhomogeneous slab. This regime involves a low-frequency approximation and holds for several experimental configurations. A review of the theory of localization for acoustic waves can be found in [217]. A remarkable application to seismic data was proposed by using an approximate expression for the localization length [308]. The following functional dependence of the localization length on the frequency has been proposed [309]:

$$\mathcal{L}(f) = C_1 + \frac{C_2}{f^2}, \tag{7.6}$$

where C_1 and C_2 are constants characterizing the medium; C_1 corresponds to the high-frequency limit, for which a lower bound of the extinction is given by taking into account only the product of all transmission coefficients of the primary pulse at every interface, which are independent of the frequency. The $1/f^2$ divergence of $\mathcal{L}(f)$ at low frequency can be intuitively explained by Rayleigh scattering. The important theoretical contribution was to show that C_2 can be computed from the correlation function of the fluctuations of compressibility [309]. As an illustration, for the case of nonstationary fluc-

tuations of the medium characterized locally by an exponential correlation function, one obtains

$$C_2 = \frac{v_0^2}{2\pi^2} \frac{1}{\int_0^L c(z) \langle \sigma^2(z) \rangle \, \mathrm{d}z} , \tag{7.7}$$

where $c(z)$ is the velocity correlation length of the small-scale inhomogeneity around the depth z and $\langle \sigma^2(z) \rangle$ is the relative variance of the compressibility. The second term in the right-hand side of (7.6) is interpreted as the contribution of multiple scattering in the forward direction. In this way it is possible to delineate almost explicitly the part played by the two competing physical process at work: single scattering and multiple forward scattering. Similarly, it was found that the spectrum of the backscattered field is directly related to the localization length. This simple formulation has been confirmed by numerical tests.

Time-domain properties of a propagating acoustic pulse have been studied under the scaling condition (7.5) in a layered medium with strong velocity perturbations, in 1D (the incident-plane-wave case) [310, 311]. It was demonstrated that propagation through the layered medium results in a time convolution of the incident pulse by a Gaussian distribution, whose variance increases with the travel time.

7.2.2 Elastic Waves

As was stated in Sect. 7.1, seismology actually deals with elastic waves rather than with scalar waves. A recent study [312] discusses a localization theory for fully elastic waves in a randomly layered medium. The evolution of the field can be described through two quantities. As for scalar waves, the localization length characterizes the spatial decay of the mean amplitude of the incident wave when propagating through the stack of random layers. The second quantity is the equilibration length, giving the characteristic length scale beyond which the ratio between the energies of compressional and shear waves tends to a constant. The existence of this equilibrium is a very important result, which will be discussed below. It is related to the nonsymmetric scattering coefficients from P to S and S to P waves, as expressed by (7.2).

The previous discussion concerned the restricted case of waves propagating in a stack of flat layers. This configuration was chosen to enable a rigorous mathematical treatment of the problem, at least under the scaling condition (7.5).

A similar configuration can be encountered in seismic prospecting in a sedimentary basin when waves reflected by a deep reflector are observed at the surface after having passed through a stack of thin layers, or when downgoing waves are recorded along a borehole in a vertical seismic-profile configuration. The signals generated by earthquakes are in most cases recorded at distances of several tens of kilometers, and therefore the wavefield propagates

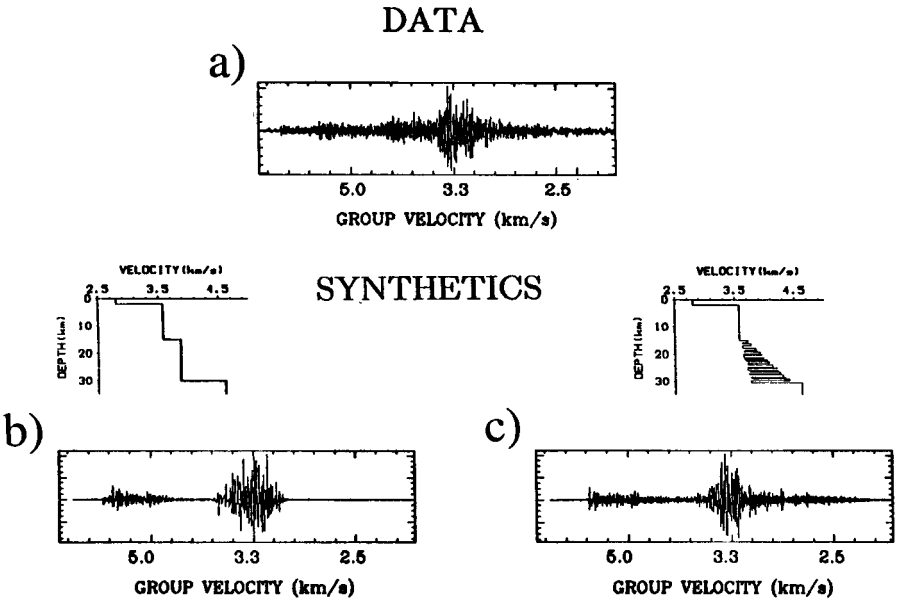

Fig. 7.1. (a) Example of a regional record of an earthquake at a distance of 386 km. The vertical ground velocity is plotted as a function of the group velocity. (b) Synthetic seismogram (*bottom*) computed for a three-layer crustal model (*top*). (c) Synthetic seismogram (*bottom*) computed for a crustal model with a thinly layered lower crust (*top*). The coda waves with low group velocities are associated with elastic leaky modes of the thin layering

in various types of geological structures in which the flat layering cannot always be regarded as a realistic approximation. Nevertheless, radiation from point sources in a 1D model has been successfully used for the study of surface waves or guided waves. As an example we present in Fig. 7.1a an actual seismogram recorded at regional distance. The records consist of the vertical ground-motion velocity. Because of the strong increase of wave velocity with depth in the shallow part of the Earth, the propagation of energy is at this distance almost horizontal, in the form of guided waves. The high-amplitude wave packet is a shear wave guided in the upper 30 km (the Earth's crust), which is called "Lg" in the seismological literature and has been extensively used in monitoring nuclear explosions. A complete numerical computation for a three-layer flat structure produces the right amplitude and time of onset of the wave train, in spite of the extreme oversimplification of the Earth structure (Fig. 7.1b). The main discrepancy between the observations and synthetics concerns the late part of the seismograms. The slowly decaying tail in the observation is the seismic coda. It is absent in the synthetics since it is produced by multiple scattering of elastic waves in the Earth. A series of flat layers with alternating high and low velocities is a crude representation of the laminations in the lower crust revealed by deep seismic soundings. The

model used in Fig. 7.1c is derived from an analysis of the filtering effect of the lower crust on deep reflections [313]. It is important to notice the strong increase of signal duration due to the presence of the layering at the base of the waveguide. This effect does not exist for scalar waves and is not predicted by a normal-mode representation of the guided elastic waves [314]. This early coda is the result of the contribution from leaky modes resulting from the multiple conversions of the field when it is scattered in the thin layering. This phenomenon is a special property of elastic waves guided in a stack of flat layers.

7.3 Seismic Coda

The most spectacular evidence of seismic scattering in the Earth is the long duration of seismic signals for local earthquakes recorded in a frequency range between 1 and 10 Hz. This duration greatly exceeds the travel time of direct paths. The late arrivals build up the "seismic coda" and this could be referred to as the "deep coda" in the case of earthquake data, a term that indicates its origin in the deep layers. It has been shown by Aki and Chouet [315] that the decay with time of the coda envelope is a constant regional characteristic, independent of the precise location of the station or of the earthquake, or of the earthquake magnitude. According to [316] this property of stationarity is observed for lapse times larger than twice the travel time of direct shear waves t_S. This rule of thumb has been widely used in coda studies, but it cannot be applied to the case where the source–receiver distance is smaller than the characteristic scale of the scattering process, i.e. the mean free path. The analysis of the seismic field using an array of seismometers indicates that the coda waves consist of shear waves coming from almost all directions. Array analysis can also be used in a reciprocal configuration [317]. In this case an "array" of earthquakes at depth is observed at the Earth's surface. This technique makes it possible to analyze the take-off of the waves at the source. Its application showed that only the early coda is made of waves scattered in the vicinity of the recorder (i.e. close to the surface), while after two or three times t_S the coda waves leave the source in a wide variety of directions [318].

The first attempt to interpret the time decay was to consider the coda waves in the framework of single scattering. For the simplest case of a homogeneous background, the scalar approximation and a receiver close to the source, the energy density for a frequency f at a lapse time t can be written as [315]

$$E(f,t) = \frac{S_0(f) g_\pi(f)}{2\pi\beta^2 t^{2\gamma}} \exp\left(-\frac{2\pi f t}{Q_c}\right), \tag{7.8}$$

where $S_0(f)$ is the shear energy emitted by the source, $g_\pi(f)$ is the backscattering coefficient and β is the shear wave velocity; γ is a factor of spreading depending upon the type of wave considered (0.5 for surface waves and 1

for body waves). Q_c, the "coda quality factor", expresses the energy decay due to scattering and inelastic processes. This expression has been widely used to characterize observations, and Q_c has emerged as a very stable parameter that seems to be correlated with the tectonic setting of the region where the measurement is done (see [319] for a review of early work on Q_c). The interest of seismologists in Q_c stems from the fact that except for Q_c, all measurements of the amplitude or attenuation of high-frequency (direct) waves are very difficult in the Earth's crust owing to focusing, defocusing and interference effects. The physical meaning of Q_c is nevertheless not clear, since the model is very crude (scalar waves in a homogeneous background) and the parts played by scattering and inelasticity are difficult to separate.

From a theoretical point of view, one expects the single-scattering model to be valid for short lapse times. The model has been refined by taking into account a finite source–receiver distance [320]. Finite-difference computations [321] have demonstrated the validity of the single-scattering model for weak heterogeneity in a 2D medium. Seismologists have made extensive use of the Born approximation, including refinement of the classical Chernov approach, for the evaluation of the extinction coefficient of transient signals in the presence of weak heterogeneity [322]. From these various studies, it emerges that for short-period seismic waves the scattering mean free path is in general of the order of tens of kilometers, a value that is intermediate between the wavelength (kilometers) and the total travel distance (a few hundreds of kilometers).

After considering the problems inherent in the phenomenological model of single scattering and the difficulties of computation in 3D with the wave equation, Wu used the stationary radiative transfer equation to obtain the total seismic energy [323]. He gave a solution for the evolution of the total energy with distance from the source for scalar waves in a homogeneous background.

These results have been used to separate the inelastic and scattering parts of the attenuation. Measurements in different regions of the world [324, 325] lead to very different figures for the ratio between intrinsic and scattering extinction lengths. In some cases these interpretations lead to very small values of the albedo which are almost in contradiction with the very existence of the coda.

An integral form of the transport equation can be introduced for isotropic scattering, in the form of a scattered-energy equation:

$$E(\mathbf{r},t) = E_{\text{in}}\left(t - \frac{|\mathbf{r}-\mathbf{r}_0|}{\beta}\right) \frac{\exp(-\eta|\mathbf{r}-\mathbf{r}_0|)}{4\pi|\mathbf{r}-\mathbf{r}_0|^2} + \int_V \eta_s E\left(\mathbf{r}_1, t - \frac{|\mathbf{r}_1-\mathbf{r}|}{\beta}\right) \frac{\exp(-\eta|\mathbf{r}_1-\mathbf{r}|)}{4\pi|\mathbf{r}_1-\mathbf{r}|^2}\,\mathrm{d}\mathbf{r}_1\,, \tag{7.9}$$

where E_{in} is the incident energy and η_s is the scattering coefficient; η is the total attenuation coefficient, which includes scattering and absorption. This

equation has been solved for high-order scattering [326]. This formulation made clear to seismologists the closeness between the ray-theory and energy-transport approaches.

Gusev and Abubakirov [327] were the first to apply a Monte Carlo simulation of the time-dependent radiative transfer equation to seismology. While limited to scalar waves in a homogeneous medium, their computation showed the transition from single scattering to multiple scattering, towards the diffusion regime. Hoshiba's Monte Carlo simulation confirms the theoretical results of Wu for the total energy [328].

7.3.1 Inhomogeneous Diffusion Models

So far, the background model has been supposed to be homogeneous. This is a serious limitation for applications to the Earth, since the average velocities are known to vary strongly with depth, resulting in strong reflections and guided propagation. The transition between the low-velocity crust and the high-velocity mantle occurs at a depth of 30 to 40 km beneath the continents, where most of the data have been collected. On the other hand, it is expected that the density of scatterers (the heterogeneity) decreases with depth. In order to study the role played by the velocity change, we solved the radiative transfer equation by the Monte Carlo technique, taking into account the reflection at the base of the crust [329]. Three models were presented. The computations correspond to isotropic scattering with a mean free path of 30 km and a diffusion constant of 35 km^2/s. The first case is a homogeneous half, space with a uniform distribution of scatterers. In the second model ("Layer 1"), the scatterer distribution is limited to a depth of 40 km in a homogeneous background. In the third model ("Layer 2"), a velocity jump is added at the same depth of 40 km to account for the S-wave velocity contrast between the crust and the mantle (3.5 km/s and 4.7 km/s respectively). The envelopes of the scattered energy at a distance of 100 km from a surface point source are presented in Fig. 7.2. In addition to the Monte Carlo results, the solutions of the diffusion equation corresponding to each model have been computed. These solutions (or their leading terms) are shown as smooth lines in Fig. 7.2. In every case, there is good agreement between the radiative-transfer-equation and diffusion solutions for large lapse times. The early part of the envelope is enlarged to show the onset of critically reflected waves in the model Layer 2. Later on, these waves tend to trap a part of the scattered energy in the crust. This is why the envelope has a much slower decay in the presence of a velocity jump (Layer 2) than in a homogeneous half-space (Layer 1). As shown in the figure, the solution of the diffusion equation provides a very good expression for the asymptotic behavior of the transfer equation. The functional forms in the diffusive regimes are the following, for $t \to \infty$:

$$\text{halfspace}: \quad E(t) \propto t^{-3/2} \tag{7.10}$$

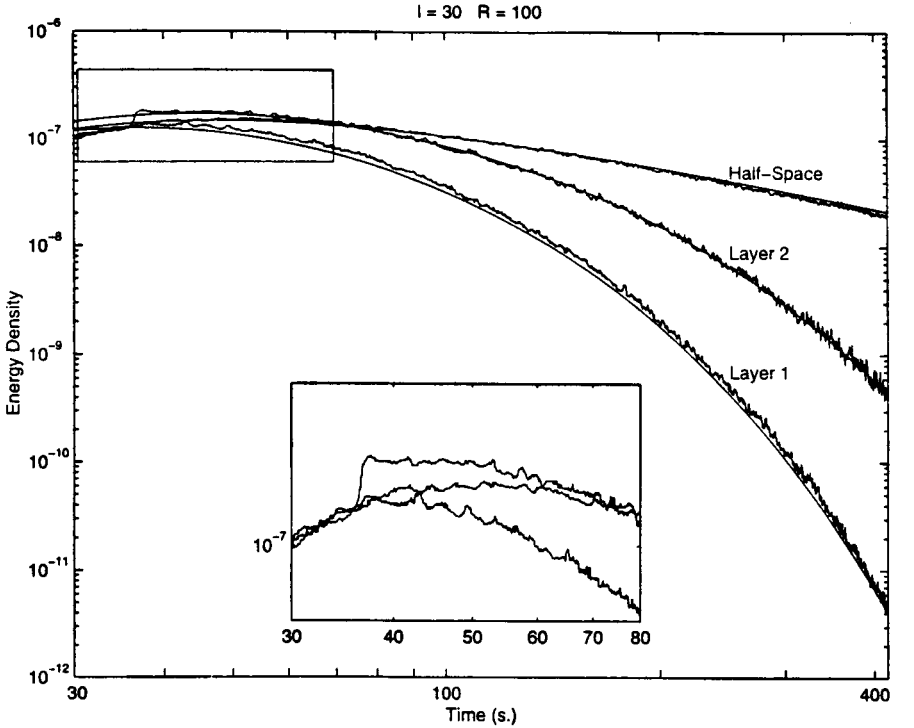

Fig. 7.2. Comparison of the results for a half-space and the models "Layer 1" and "Layer 2". The solutions of both the radiative transfer and the diffusion equation are shown. The former exhibits the ripples characteristic of the Monte Carlo method used. The source–station distance is $R = 100$ km and a mean free path $\ell^* = 30$ km has been adopted in all models. For Layer 1 and Layer 2, scattering is confined to a slab of thickness $H = 40$ km. In the half-space model and Layer 1, the S-wave velocity is uniform and equal to 3.5 km/s, whereas Layer 2 includes a velocity jump at depth H. The time origin is time of the release of energy at the source. The beginning of the signals is magnified (*inset*) in order to distinguish the evolution of the coda in the three models

$$\text{Layer 1 and Layer 2}: \quad E(t) \propto \frac{\exp(-Dt\xi_0^2/H^2)}{HDt}. \tag{7.11}$$

Here D is the diffusion coefficient and H is the thickness of the layer; ξ_0^2 is a variable depending upon H and D in a homogeneous background (model Layer 1), while it is also a function of the reflection coefficient in the presence of a velocity contrast (model Layer 2) [329]. The half-space model does not predict the observed behavior in (7.8), which indicates a faster decay of energy with time. In the case of the models Layer 1 and Layer 2, the expression for the asymptotes of the envelopes is formally similar to the one proposed to fit the observations (7.8) and therefore makes it possible to give a physical interpretation of Q_c in terms of long-range diffusion with bottom leaks. A

quantitative analysis with realistic values shows that the model Layer 1 leads to too rapid a decay of the envelope with respect to the observations. When the reflected waves are taken into account (model Layer 2), the decay is close to that observed [329], even for the perfectly elastic model considered here. Typically, if one interprets the curve shown in Fig. 7.2 for the model Layer 2 in terms of (7.8), the Q for the coda is found to be frequency-dependent in the form $Q_c = 230f$, which is definitely in the range of proposed values in areas of active tectonics. This suggests that the albedo of the Earth's crust is much larger than the values proposed using models with a uniform distribution of scatterers.

7.3.2 Role of Polarization

In the previous discussion it was assumed that coda waves consist of shear waves and that P to S and S to P conversions can be neglected. This assumption was suggested by (7.2). More generally, the transport equation can be modified into two coupled equations for the P and S energies by taking into account the coupling using the single-scattering result of (7.2) [330, 331]. More detailed theoretical discussions that consider the coupled equations for the P-wave energy and the coherence matrix of the transversely polarized shear waves have been given by Weaver [332] and Ryjhik et al. [333].

For an elastic wave, we have to define the scattering mean free paths associated with four different types of scattering: PP, SS, PS and SP. For each case, the mean free path ℓ^{XY} is given by the usual definition,

$$\frac{1}{\ell^{XY}} = \int_{-1}^{1} \sigma^{XY}(\cos\theta)\, \mathrm{d}\cos\theta\,, \tag{7.12}$$

where θ is the angle between the incident and scattered waves and σ^{XY} is the differential cross-section for scattering of type XY, XY being PP, SS, PS or SP. The corresponding attenuation coefficient is given by $\Sigma^{XY} = 1/\ell^{XY}$. The total scattering mean free paths or reciprocal attenuation coefficients can be written as

$$\frac{1}{\ell^{\mathrm{P}}} = \frac{1}{\ell^{\mathrm{PP}}} + \frac{1}{\ell^{\mathrm{PS}}}\,, \tag{7.13}$$

$$\frac{1}{\ell^{\mathrm{S}}} = \frac{1}{\ell^{\mathrm{SS}}} + \frac{1}{\ell^{\mathrm{SP}}}\,. \tag{7.14}$$

Recalling the relation (1.13), a relevant quantity is the forward weighted scattering attenuation coefficient [334]

$$\Sigma^{*XY} = \int_{-1}^{1} \sigma^{XY}(\cos\theta)\cos\theta\, \mathrm{d}\cos\theta. \tag{7.15}$$

This quantity vanishes if forward scattering and backscattering have equal probability and is intimately related to the transport mean free path as defined in optics according to (1.13). Since for each wave type the transport

mean free path describes the effect of both diffraction and mode conversion, its value cannot be deduced from the mean free path and the mean cosine of a scattering angle as for scalar waves. When there is no preferential scattering (all $\Sigma^{*XY} = 0$), the transport mean free path is equal to the mean free path, as for scalar waves. In the general case of preferential scattering [332], two transport mean free paths can be defined as

$$\ell^{P*} = \frac{\Sigma^{S} - \Sigma^{*SS} + \Sigma^{*PS}}{(\Sigma^{P} - \Sigma^{*PP})(\Sigma^{S} - \Sigma^{*SS}) - \Sigma^{*PS}\Sigma^{*SP}},$$
$$\ell^{S*} = \frac{\Sigma^{P} - \Sigma^{*PP} + \Sigma^{*SP}}{(\Sigma^{P} - \Sigma^{*PP})(\Sigma^{S} - \Sigma^{*SS}) - \Sigma^{*PS}\Sigma^{*SP}}. \tag{7.16}$$

A striking feature that appears to be a universal property has been pointed out for the diffusive regime [333, 334]. For long lapse times when the diffusion approximation is valid, the theory predicts that, independently of the details of the scattering, the energies of the P and S waves tend to equilibrate at a constant ratio:

$$\frac{E^{P}}{E^{S}} = \frac{\beta^3}{2\alpha^3}. \tag{7.17}$$

This important property remains to be confirmed by observations; it is also predicted in nematic liquid crystals [31]. The transition to the diffusive regime has been studied using a Monte Carlo simulation for elastic waves in the framework of ultrasound propagation [334]. It appears that the equilibrium between compressional and shear energy is preceded by an intermediate stage in which the shear component tends to become isotropic. The diffusion coefficient for elastic waves, D_e, is given by

$$D_e = \frac{\beta \ell^{S*}}{3}\left(\frac{\alpha \ell^{P*}/\beta \ell^{S*} + 2(\alpha/\beta)^3}{1 + 2(\alpha/\beta)^3}\right). \tag{7.18}$$

For actual applications in seismology, the consideration of elastic waves makes a significant difference from the case of the scalar approximation. With realistic values the elastic diffusivity is about 50 % higher than the shear-only diffusivity [334].

7.4 Coherent Backscattering and Localization in Seismology

Except for the case of sedimentary (1D) layering, localization of seismic waves has so far not been demonstrated theoretically. The coherent backscattering cone, often believed to be a precursor of strong localization, has not been observed. The coherent backscattering cone is a phenomenon resulting from an interference between reciprocal paths that occurs in the exact direction of the incident wave, with a perfect amplitude-doubling in the case where

reciprocity applies perfectly. In an elastic body such as the Earth, the scattering process includes the coupling between the two different wave types described above. Therefore the scattered field is made up of contributions from both P and S waves. The reciprocity principle cannot be invoked for the part of the field which is not of the same type as the incident wave, even in the specular direction. This suggests that the magnitude of this effect will be smaller for elastic waves than for scalar waves. From a practical point of view, the controlled sources of high energy are explosions, whose primary radiation is essentially P-like, whereas the scattered waves are essentially S-like, as emphasized before. This particular fact makes it difficult to realize an experiment that allows a direct measurement of the amplitude of the cone.

Coherent backscattering of elastic waves from a rough boundary has been computed numerically by Schultz and Toksoz [335, 336]. To obtain stabilization of the speckle, it was necessary to perform a configuration average over a large number of realization of the interface geometry. Such an averaging is very difficult to realize with actual data since self-averaging is not expected in reflection.

The analysis of seismological data shows that narrow regions exist in which the coherent shear waves disappear almost completely, while there is no evidence or indication of a strong intrinsic attenuation. The existence of extreme heterogeneity has been invoked to explain these extinctions [337].

The coda waves recorded during local earthquakes on the volcanic island of La Réunion by an array of seismometers show an intriguing behavior that seems to indicate some form of localization [338]. The situation in La Réunion is exceptional, with the presence of a magmatic zone which is known to be extremely heterogeneous and to have a high average velocity. This last point excludes the existence of trapped modes inside the magmatic zone. The local amplification factor associated with each station was computed from the coda wave amplitude at a long lapse time (70 s). The frequency band considered was 1–3 Hz. These amplification factors have been shown to correspond to the response of shallow layers beneath the station [339], and do not exhibit any systematic geographic dependence. The travel time t_S of direct waves in this experiment depends on the earthquake and is typically less than 10 s. One would expect that normalization done using the amplification factor would be effective for lapse times larger than $2t_S$, according to numerous observations around the world. A major departure from this usual behavior has been observed in La Réunion. To visualize this, the amplitude of the coda waves in the time window 30–40 s was corrected using the amplification factor and normalized with respect to a reference station. The distribution of the normalized coda amplitude shows a maximum, and a smooth decrease around the maximum. For all earthquakes, the maximum corresponds to the axis of the volcano, while some of the earthquakes are located far away. From the spread of this maximum (about 5 km) at a lapse time of 35 s, a rough estimate of the diffusion coefficient can be proposed. With the simple assumption of

scalar transport theory, the transport mean free path can be evaluated. With the values obtained in this study, ℓ^* is found to be very short: of the order of 360 m. This is significantly smaller than the wavelength (about 1 km) and by the Ioffe–Regel criterion (1.20), localization concepts may be necessary to explain the observations.